Tropical Cyclone Intensity Change from a Simple Ocean–Atmosphere Coupled Model

JOHNNY C. L. CHAN AND YIHONG DUAN*

Department of Physics and Materials Science, City University of Hong Kong, Hong Kong, China

LYNN K. SHAY

Division of Meteorology and Physical Oceanography, Rosenstiel School of Marine and Atmospheric Science, University of Miami, Miami, Florida

(Manuscript received 28 May 1999, in final form 13 May 2000)

ABSTRACT

The interaction between a tropical cyclone (TC) and the underlying ocean is investigated using an atmosphere–ocean coupled model. The atmospheric model is developed from the Pennsylvania State University (Penn State)–National Center for Atmospheric Research (NCAR) mesoscale model version 4 MM4 and the ocean model consists of a mixed layer and an inactive stagnant layer beneath. Coupling between the atmosphere and the ocean models is achieved through wind stress and surface heat and moisture fluxes that depend on the sea surface temperature (SST). In the absence of a background flow, the atmospheric component consists of only a predefined vortex with an initial central pressure and the radius of the 15 m s^{-1} wind. The basic control experiments demonstrate that the coupled model can simulate the development of a TC and its interaction with the ocean.

Changes in TC intensity are sensitive to those of SST and the response is almost instantaneous. An SST of ~27°C is found to be the threshold for TC development. In addition, the initial depth of the ocean mixed layer has an appreciable effect on TC intensity, which also depends on the movement of the TC. Furthermore, the vertical structure of ocean (vertical temperature gradient in the stagnant layer and temperature differential between the two layers) plays a significant role in modulating TC intensity.

In the presence of a warm core eddy (WCE), a TC intensifies before its center reaches the edge of the WCE. Although the TC attains maximum intensity at the center of the WCE, it does not weaken to its original intensity after leaving the WCE. During the entire passage of the TC, the SST at the center of the WCE decreases by about only 1°C, and the WCE generally maintains its original characteristics. However, two cold pools are observed around its periphery. A similar intensification process occurs when a TC moves over a sharp SST gradient and a locally deep ocean mixed layer. These results are explained by the interaction between the ocean and the TC circulation as well as the change in the total surface heat flux.

1. Introduction

Previous studies have shown that synoptic-scale conditions and sea surface temperature (SST) tend to control the development of a tropical cyclone (TC) (e.g., Gray 1979; Emanuel 1988; Demaria and Pickle 1988). Many other studies (Holland and Merrill 1984; Molinari and Vollaro 1990; Ross and Kurihara 1995; Willoughby and Black 1996) also indicate that the internal dynamics and thermodynamics of the TC can affect its track and intensity.

In early numerical TC–ocean interaction studies (Elsberry et al. 1976; Chang and Anthes 1978; Sutyrin and Khain 1979), an axisymmetric TC model was coupled to an ocean mixed layer model. The results suggest that the simulated interaction is small probably because of the coarse resolution. Ginis et al. (1989) developed a three-dimensional air–sea interaction model by coupling a five-level TC model (Khain 1988) with a three-layer primitive equation ocean model (Ginis and Dikinov 1989). Both the increased intensity and movement of the modeled TC resulted in a cooling of the sea surface. Bender et al. (1993) applied the high-resolution coupled model of the Geophysical Fluid Dynamics Laboratory to study idealized TC–ocean interactions. They found that the TC-induced cooling of the sea surface has a significant impact on the ultimate storm intensity, due to the reduction of total heat flux directed into the TC. Hodur (1997) also obtained similar results from the Coupled Ocean/Atmosphere Mesoscale Prediction System developed by the Naval Research Laboratory.

* Additional affiliation: Shanghai Typhoon Institute, Shanghai, China.

Corresponding author address: Johnny Chan, Dept. of Physics and Materials Science, City University of Hong Kong, 83 Tat Chee Ave., Kowloon, Hong Kong, China.
E-mail: Johnny.Chan@cityu.edu.hk

TABLE 1. Values of various parameters of the control experiment (expt. A0), and two basic experiments (expts. AC and B0).

Parameter	Expt. A0	Expt. AC	Expt. B0
Central pressure (hPa)	986	986	986
Radius of 15 m s^{-1} winds (km)	250	250	250
Initial SST (°C)	27	27	27
Initial ML depth (m)	—	50	50
Basic mean flow (m s^{-1})	No	No	5.0
Coupled	No	Yes	No

In most of these experiments, the feedback process of the ocean to a TC is studied mainly in terms of the changes in the TC intensity and track. It is generally agreed that the impact of the ocean on TC intensity and track is through surface heat fluxes. Since the distribution of the heat fluxes is determined by the SST and the ocean mixed layer depth, the feedback mechanisms depend on the vertical structure of the upper ocean. A more detailed investigation is therefore necessary to examine the processes that modulate the SST and surface heat fluxes. Neither of these latter two parameters is spatially uniform given the spatial variability in oceanic fronts and eddies. Over the oceans where TCs traverse, warm pools [such as the warm ocean eddy found by Shay et al. (2000), associated with the rapid intensification of Hurricane Opal (1995)] or large SST gradients (such as the Gulf Stream or the Kuroshio Current) are often found. A key question is whether such effects on TC intensity can be simulated and understood in terms of the interaction between the ocean and the TC circulation. The objective of the present paper is therefore to study changes in the intensity and structure of a TC under differing, yet realistic, ocean conditions and the associated oceanic response within the context of a simple coupled model.

Section 2 provides a brief description of the ocean–atmosphere coupled model. Results from the control experiments for verifying the ability of the model to simulate the evolution of a TC and that of the underlying ocean are shown in section 3. Intensity changes of a TC under different ocean conditions are studied in section 4. These include variations in SST and the vertical structure of the ocean, and passage of a TC over various local areas of inhomogeneities [a warm core eddy (WCE), a locally deep ocean mixed layer, and a sharp gradient of SST]. Results are summarized in section 5, where some concluding remarks are also given.

2. Brief description of the model

a. Atmospheric model

The atmospheric model was developed from the Pennsylvania State University (Penn State)–National

TABLE 2. List of experiments conducted.

Experiment name	Description
SST changes (as in Expt. AC except for)	
Expt. S1	SST = 25°C after 6 h
Expt. S2	SST = 26°C after 6 h
Expt. S3	SST = 28°C after 6 h
Expt. S4	SST = 29°C after 6 h
Expt. S5	SST = 30°C after 6 h
Expt. S6	SST = 31°C after 6 h
Changes in ML depth and mean flow (as in Expt. AC except for)	
Expt. UM01	ML depth of 100 m
Expt. UM02	ML depth of 75 m
Expt. UM03	ML depth of 25 m
Expt. UM11	ML depth of 100 m and easterly flow = 2.5 m s^{-1}
Expt. UM12	ML depth of 75 m and easterly flow = 2.5 m s^{-1}
Expt. UM13	ML depth of 25 m and easterly flow = 2.5 m s^{-1}
Expt. UM21	ML depth of 100 m and easterly flow = 5 m s^{-1}
Expt. UM22	ML depth of 75 m and easterly flow = 5 m s^{-1}
Expt. UM23	ML depth of 25 m and easterly flow = 5 m s^{-1}
Changes in vertical temperature gradient of stagnant layer (GAMMA) (as in Expt. AC except for)	
Expt. GM1	GAMMA = 0.05°C m^{-1}
Expt. GM2	GAMMA = 0.15°C m^{-1}
Expt. GM3	GAMMA = 0.20°C m^{-1}
Changes in temperature difference between the two ocean layers (DT) (as in Expt. AC except for)	
Expt. DT1	DT = 0.5°C
Expt. DT2	DT = 1.5°C
Expt. DT3	DT = 2.0°C
Localized inhomogeneities in the ocean	
Expt. P1	Passage over a warm core eddy along TC track
Expt. P2	Passage over a sharp gradient of SST
Expt. P3	Same as expt. P1, except for initially homogeneous SST

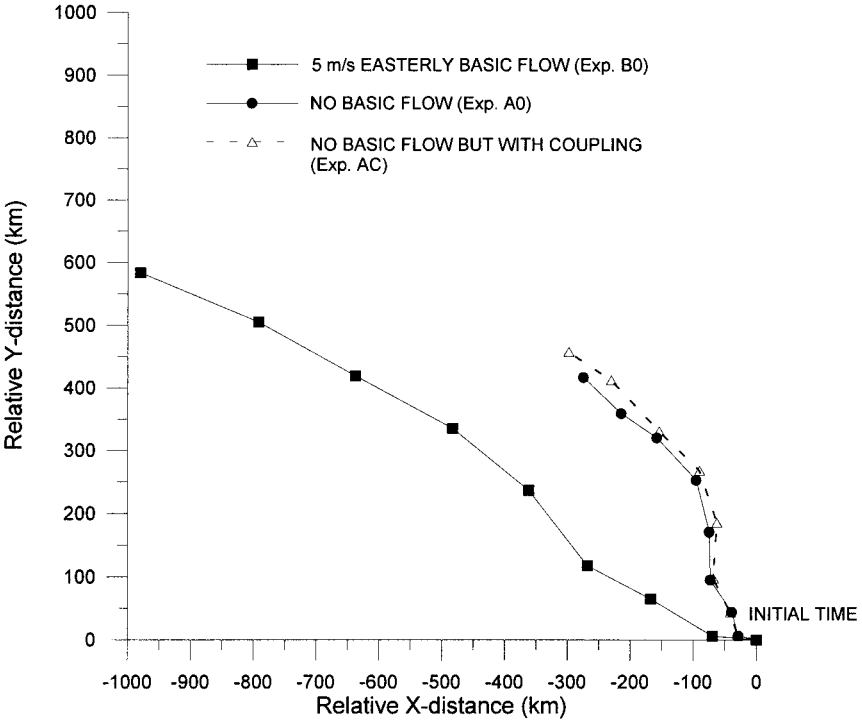

FIG. 1. TC track simulated in expts. A0, AC, and B0. The positions are 6 h apart.

Center for Atmospheric Research (NCAR) mesoscale model version 4 (MM4), details of which have been outlined in Anthes et al. (1987). It is a primitive equation model formulated on a Lambert projection and in σ coordinates, with 16 levels in the vertical. The σ levels are placed at values of 1.0, 0.98, 0.95, 0.90, 0.8, 0.65, 0.5, 0.4, 0.32, 0.26, 0.20, 0.15, 0.10, 0.06, 0.03, and 0.0. The Kuo cumulus parameterization (Kuo 1974; Anthes 1977) scheme is used. A bulk aerodynamic model of the planetary boundary layer, following Deardorff (1972), is employed, in which horizontal diffusion is second order and vertical diffusion is parameterized with *K*-theory.

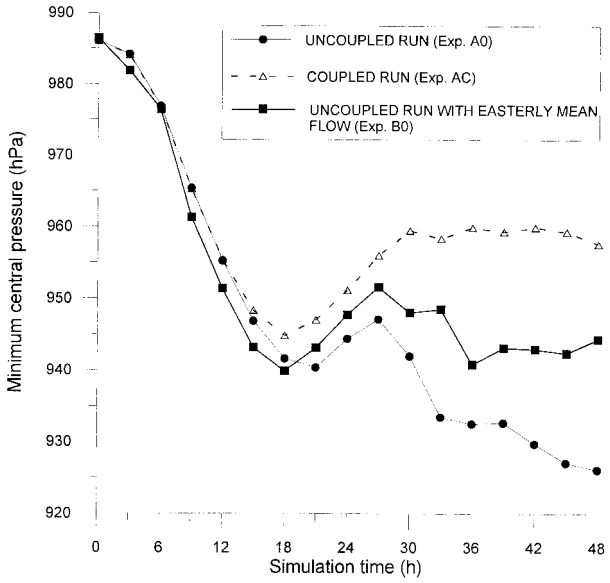

FIG. 2. Time series of minimum central pressure (hPa) of TC in expts. A0, AC, and B0.

Recently, it has been suggested that the Kuo scheme may not be appropriate for the study of mesoscale phenomena because it lacks a cloud model or convective downdrafts (Raymond and Emanuel 1993). However, Wang and Seaman (1997) compared the results of a mesoscale model using four different cumulus parameterization schemes and found the Kuo scheme to be no less accurate in terms of the overall precipitation. Peng et al. (1999) also obtained physically reasonable results using the Kuo scheme in their simulation of TC intensification. In another investigation of the effects of different cumulus parameterization schemes on the rates of TC intensification using version 5 of the Penn State/NCAR mesoscale model (MM5) coupled with the same ocean model, we found that the absolute rates can vary appreciably among the various schemes. However, the relative rates of intensification (i.e. differences in the rates for different SSTs) are very similar. An example of this is shown in the appendix. Since the main objective of the present study is to compare the effects of various ocean conditions on TC intensification and to study the physical processes associated with these effects, the result presented in Fig. A1 suggests that the choice of parameterization scheme should not have a

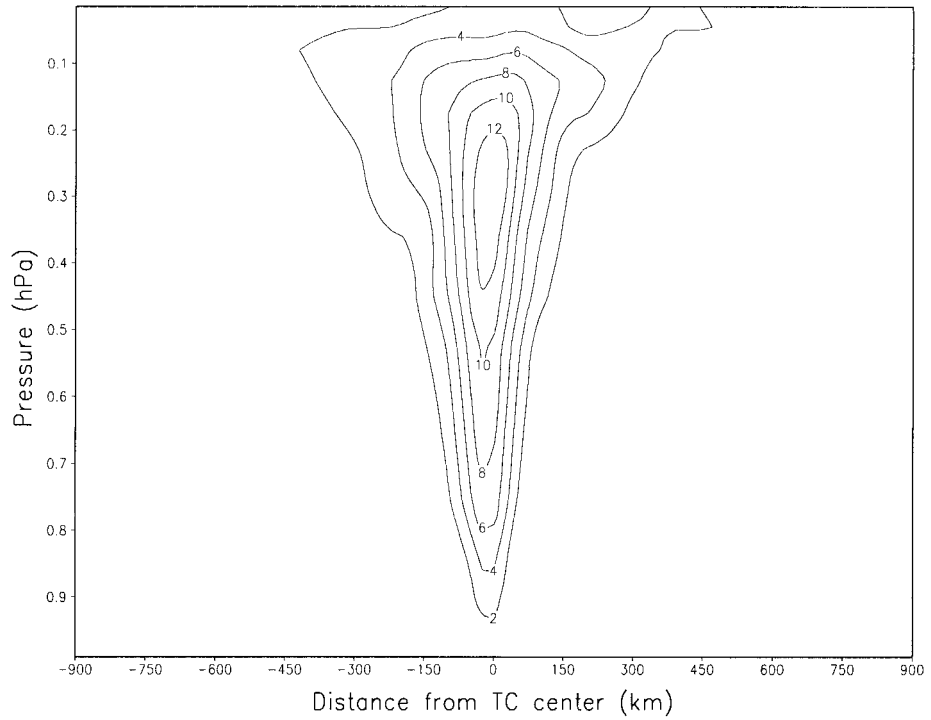

FIG. 3. Vertical east–west cross section of temperature deviations across the TC center at 48 h for expt. A0. See text regarding how the deviations are calculated. Contour interval: 2°C.

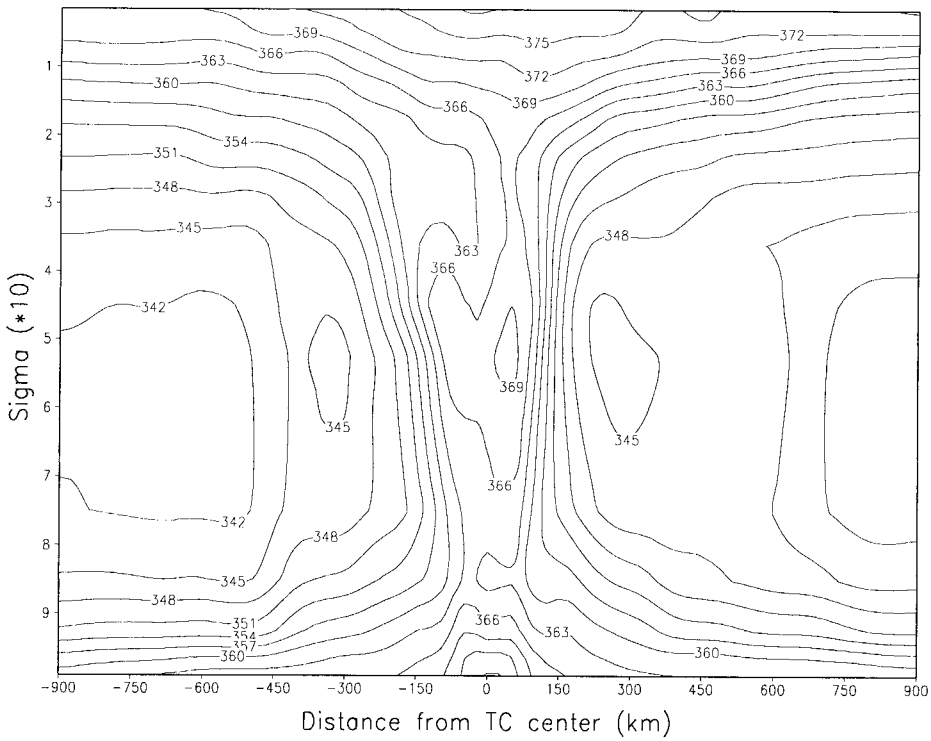

FIG. 4. As in Fig. 3, except for the equivalent potential temperature (in K) at 24 h. Contour interval: 5 K.

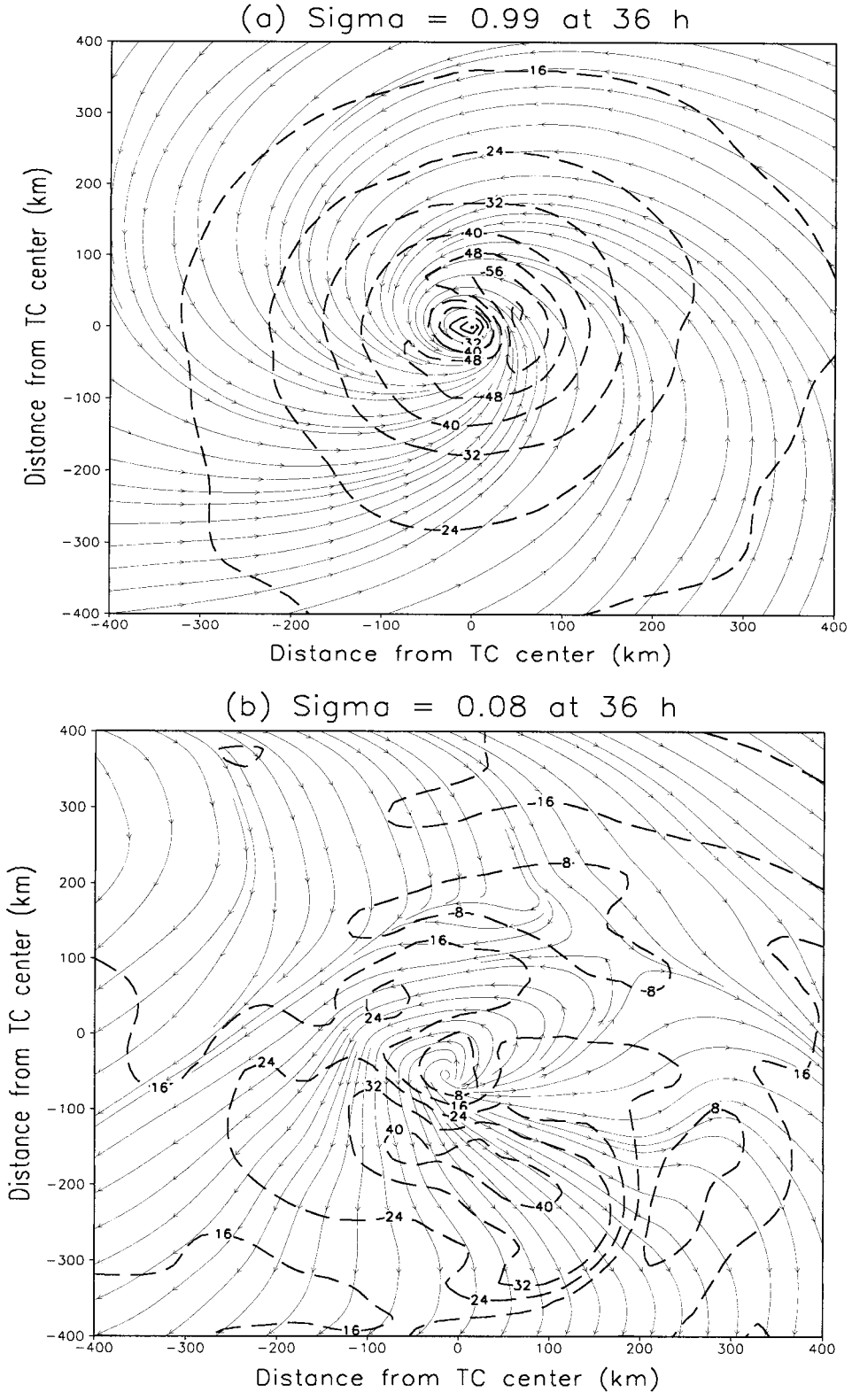

FIG. 5. Streamlines and isotachs at (a) $\sigma = 0.99$ and (b) $\sigma = 0.08$ for expt. A0 at 36 h. Isotach interval: 8 m s^{-1}.

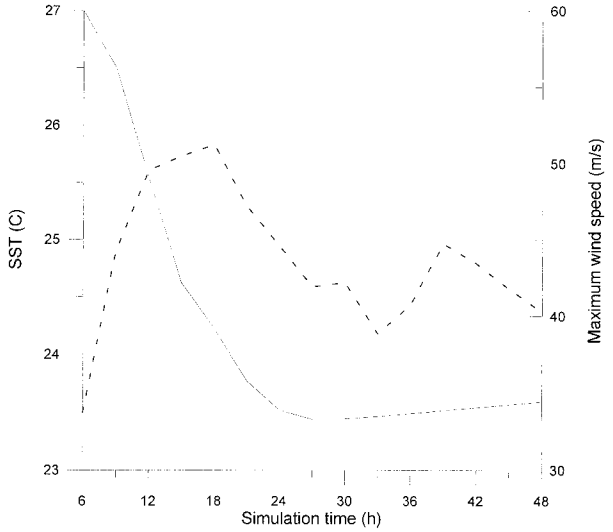

FIG. 6. Time series of minimum SST (°C) of expt. AC (solid) within the TC circulation and maximum wind speed (m s^{-1}) (dashed).

significant impact on the conclusions. Thus, it is decided that the Kuo scheme should be adequate for the present study.

Several methods for inserting a vortex into the initial fields have been designed (e.g., Kurihara et al. 1993; Heming et al. 1995; Hodur 1997). The bogus TC used in the present study is specified by the radius of 15 m s^{-1} (R_{15}) winds, the boundary radius of the TC (R_E), and the central pressure P_C. The sea level pressure at a distance, r, from the TC center, $P_{SE}(r)$, is given by Fujita's (1952) formula:

$$P_{SE}(r) = P_E - \Delta P\left[1 + \left(\frac{r}{R_0}\right)^2\right]^{-0.5},$$

where P_E is the environmental pressure, R_0 the radius of maximum wind, and $\Delta P = P_E - P_C$.

The model domain is 4900 × 4500 km, with a horizontal grid size of 25 km. The ''Arakawa B'' horizontal grid structure is used. An explicit time-integration scheme developed by Brown and Campana (1978) is employed, which allows for a time step of 30 s, about 1.6 times larger than that allowed by a conventional leapfrog scheme but that produces virtually identical results. The inflow/outflow lateral boundary conditions are used. In the vertical, $\dot{\sigma}$ is zero at $\sigma = 0$ and 1. The domain is large enough so that the boundary conditions should have little effect on predictions up to 72 h. All the variables are defined at the half-σ levels, except $\dot{\sigma}$.

b. The ocean mixed layer model

The ocean is approximated as a two-layer incompressible Boussinesq fluid that consists of a mixed layer (ML), with predicted variables of temperature, current, and layer depth, and an inactive layer below, in which the temperatures at great depths decrease linearly as a function of increasing depth. The governing equations in Lambert projection coordinates for the upper ML have the following form (Zhu 1994):

$$\frac{\partial u}{\partial t} = -mu\frac{\partial u}{\partial x} - mv\frac{\partial u}{\partial y} - \frac{1}{2}mgh\frac{\partial h}{\partial x} - m\varepsilon g\frac{\partial h}{\partial x} + fv + \frac{1}{\rho_m h}(\tau_{ax} - \tau_{bx}) + m^2 A_m\left(\frac{\partial^2 u}{\partial x^2} + \frac{\partial^2 u}{\partial y^2}\right),$$

$$\frac{\partial v}{\partial t} = -mu\frac{\partial u}{\partial x} - mv\frac{\partial v}{\partial y} - \frac{1}{2}mgh\frac{\partial u}{\partial y} - m\varepsilon g\frac{\partial h}{\partial y} - fu + \frac{1}{\rho_m h}(\tau_{ay} - \tau_{by}) + m^2 A_m\left(\frac{\partial^2 v}{\partial x^2} + \frac{\partial^2 v}{\partial y^2}\right),$$

$$\frac{\partial T}{\partial t} = -mu\frac{\partial T}{\partial x} - mv\frac{\partial T}{\partial y} + K_H m^2\left(\frac{\partial^2 T}{\partial x^2} + \frac{\partial^2 T}{\partial y^2}\right) + \frac{Q}{\rho_m C_p h} + \left(\frac{dT}{dt}\right)_m, \quad \text{and}$$

$$\frac{\partial h}{\partial t} = -m^2\frac{\partial}{\partial x}\left(\frac{uh}{m}\right) - m^2\frac{\partial}{\partial y}\left(\frac{vh}{m}\right) + \left(\frac{dh}{dt}\right)_m.$$

The definitions of the symbols are as follows:

t	time;
h	depth of the upper layer;
u, v	velocity components in the x and y directions, respectively;
g	gravity;
m	map factor;
ε	density anomaly;
f	Coriolis parameter;
ρ_m	upper-layer density;
T	upper-layer temperature;
τ_{ax}, τ_{ay}	wind stress components in the x and y directions, respectively;
τ_{bx}, τ_{by}	x and y components of stress between the layers, respectively;
Q	sea surface heat flux;
$(dT/dt)_m$, $(dh/dt)_m$	upper-layer temperature and depth change due to entrainment, respectively;
A_m, A_k	horizontal diffusion coefficients of momentum and heat, respectively.

The sea surface is flat with a rigid-lid approximation, and the effect of salinity is ignored because of its minor importance to the TC (Chang and Anthes 1978). The entrainment velocity is parameterized according to Kato and Phillips (1969) and Chang and Anthes (1978). The capability of this model to simulate the ocean currents, as well as ML temperatures and depth associated with a moving TC, has been well demonstrated in experiments using real data (e.g., Zhu 1994; Qin and Zhu 1995).

The horizontal grid spacing is 50 km. The wind forc-

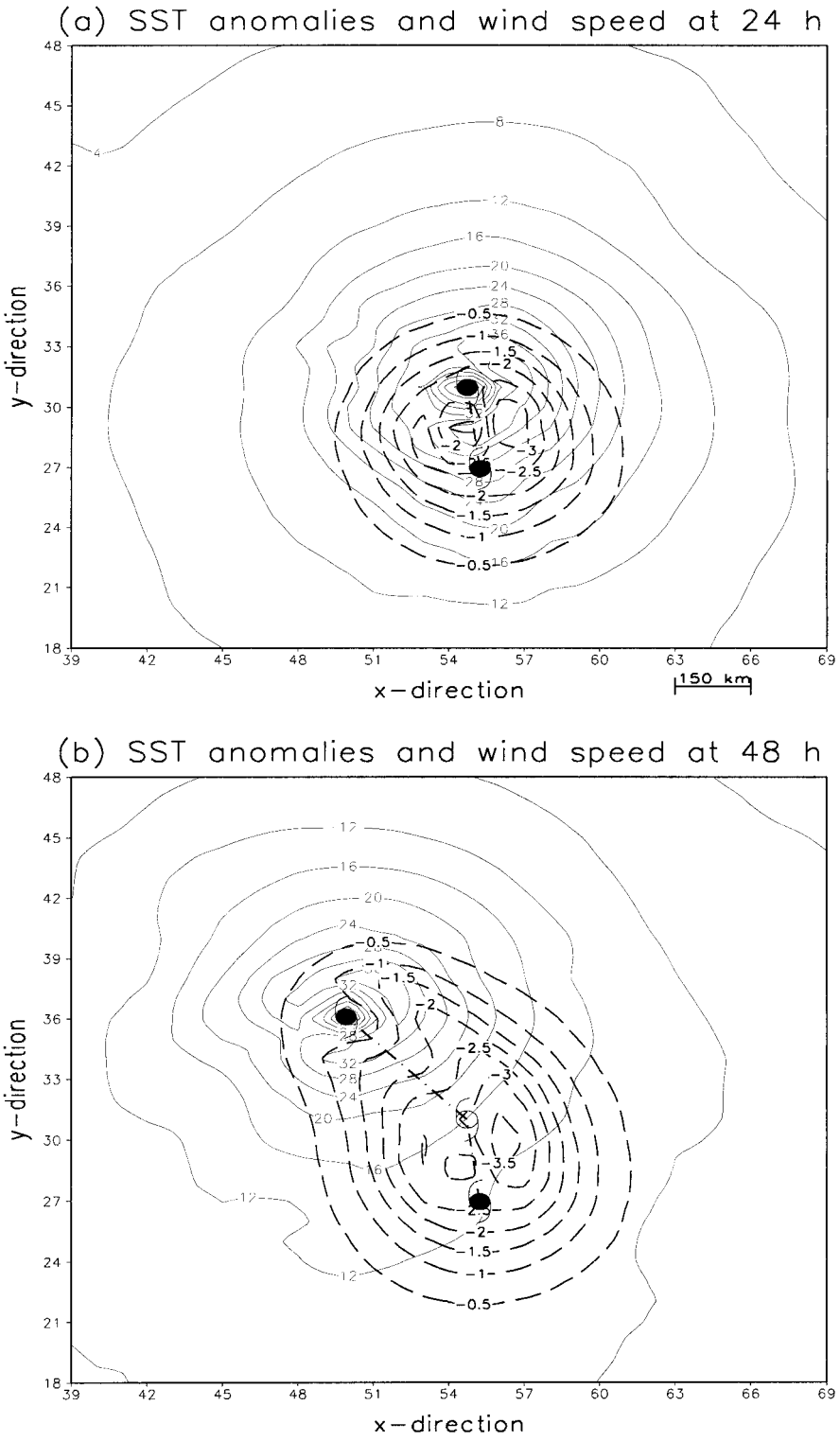

FIG. 7. Distribution of SST anomalies (dashed) and wind speeds (solid) at (a) 24 h and (b) 48 h for expt. AC. The dot-dashed line indicates the track of the modeled TC. The solid typhoon symbols indicate the initial and current positions of the modeled TC, and the empty typhoon symbol in (b) is the 24-h position. Contour interval: 4 m s^{-1} (for wind), 1°C (for SST).

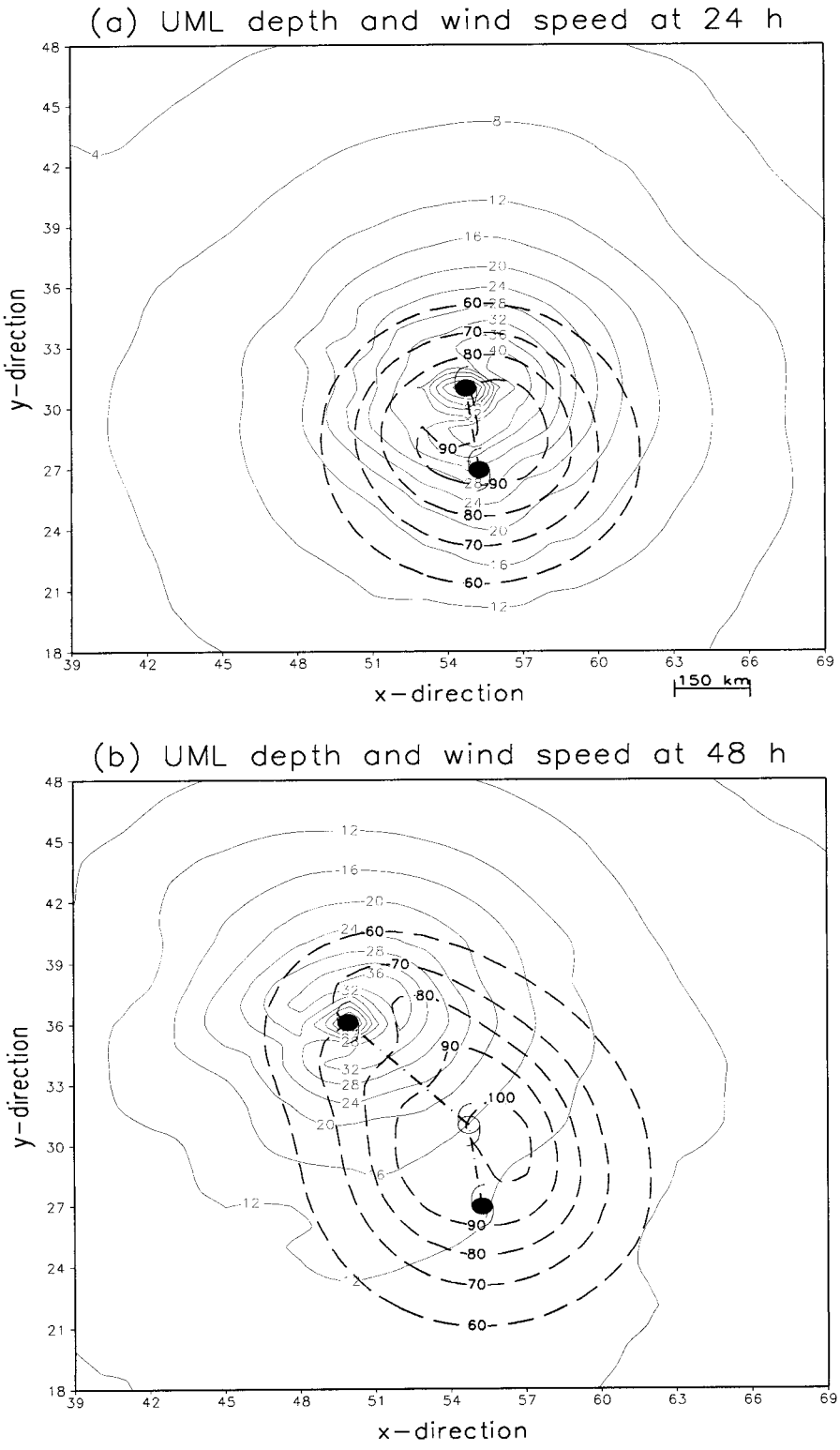

FIG. 8. As in Fig. 7, except for ML depth. Contour interval: 10 m.

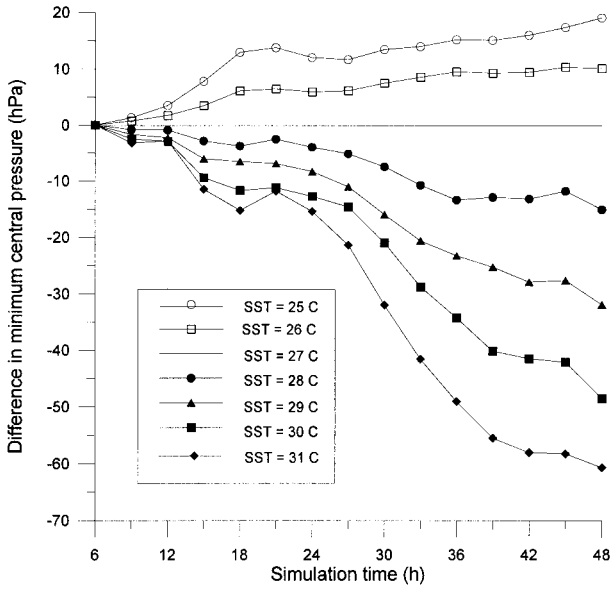

FIG. 9. Time series of the difference in MSLP (hPa) between expts. S1–S6 and expt. AC.

ing to the ocean utilizes the output from the atmospheric model interpolated to the ocean model grid at every time step. The same method is also used for providing the SST forcing from the ocean model to the atmospheric model. The leapfrog scheme is used in the ocean model with the same time step as in the atmospheric model so that they can be easily coupled.

c. Initial conditions

Generally, experiments are conducted with a prespecified vortex and a quiescent atmospheric environment. The atmosphere is homogeneous at the standard pressure levels (1000, 850, 700, 500, 300, 200, and 100 hPa). The vertical temperature structure is obtained from the European Centre for Medium-Range Weather Forecasts (ECMWF) reanalysis data (0000 UTC 21 September 1990) averaged within 135°–155°E and 10°–20°N. Because the humidity values from the ECMWF reanalysis are too dry for the model TC to grow, these values are set to 90%, 85%, 80%, 50%, 20%, 20%, and 10% at the 7 standard pressure levels from 1000 to 100 hPa, respectively. The geopotential heights at various pressure levels are calculated using the hydrostatic relationship. When a mean flow is considered, the geopotential height is calculated by geostrophic balance. The SST is also taken as homogeneous in all the control experiments with a uniform ocean ML depth of 50 m.

TABLE 4. MSLP (hPa) at 48 h in the experiments with different ML and mean basic flow.

ML depth (m)	No basic flow	$U = 2.5$ m s^{-1}	$U = 5.0$ m s^{-1}
100	937	938	948
75	948	947	953
50	957	957	960
25	972	971	971

A control experiment is first run to verify the ability of the model to produce a realistic TC (expt. A0, parameters defined in Table 1). Based on the study of Liu and Chan (1999), R_{15} is taken as 250 km for a TC with a central pressure of 986 hPa. With these parameters, the maximum winds are about 22 m s^{-1} at a radius of ~200 km. Two other basic experiments have also been carried out (Table 1). Experiment B0 is designed to check the validity of the model in the presence of an environment mean flow. Experiment AC is designed to examine the ability of the coupled model to simulate the atmosphere–ocean interaction. This experiment is integrated for 72 h and serves as a background for studying the passage of a TC over various localized oceanic anomalies.

All numerical experiments performed in this study are listed in Table 2. They will be introduced as each set of experiments is discussed. All coupled model runs begin after the atmospheric model has been integrated for 6 h, to decrease the effect of adjustment of the atmospheric model to the ocean forcing.

3. Model validation

This section presents results from three basic experiments to demonstrate that the model can indeed simulate the development of a hurricane-like vortex with and without interaction with the ocean, as well as under the influence of a mean flow. Comparisons are made with those from previous studies where appropriate. Therefore, it is important to note that these results do not represent new findings. Rather, they simply illustrate the validity of the current coupled model.

a. Uncoupled and without a mean flow (expt. A0)

The TC track from experiment A0 is northwestward (Fig. 1) with an average speed of ~3.6 m s^{-1}. This self-propagation generally agrees with the β effect previously identified for a relatively large vortex (e.g., Chan and Williams 1987). Such a propagation in the absence of an environmental flow has also been simulated by other ocean–atmosphere models (e.g., Bender et al.

TABLE 3. Rate of change in TC intensity with respect to SST at 48 h.

Range of SST (°C)	25~26	26~27	27~28	28~29	29~30	30~31
Rate of MSLP with SST (hPa °C^{-1})	8.9	10.1	15.7	16.7	16.7	12.2

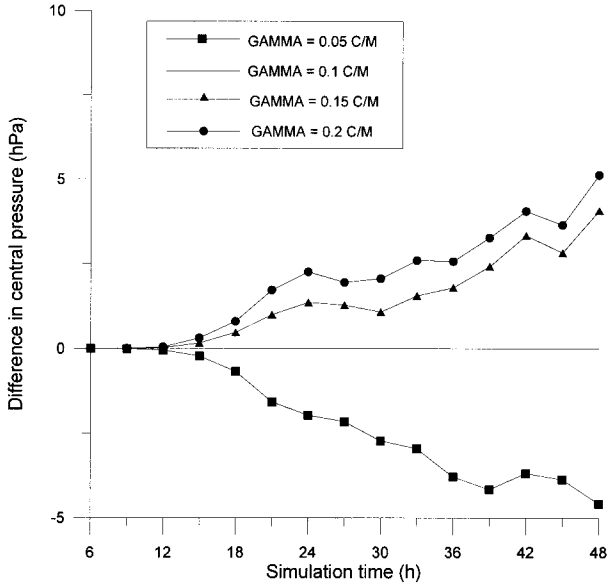

FIG. 10. Times series of the difference in MSLP (hPa) between three experiments [expt. GM1 (GAMMA = 0.05°C m^{-1}), expt. GM2 (GAMMA = 0.15°C m^{-1}), and expt. GM3 (GAMMA = 0.2°C m^{-1})] and expt. AC (GAMMA = 0.1°C m^{-1}). Value of GAMMA is the vertical temperature gradient of the stagnant layer in the ocean.

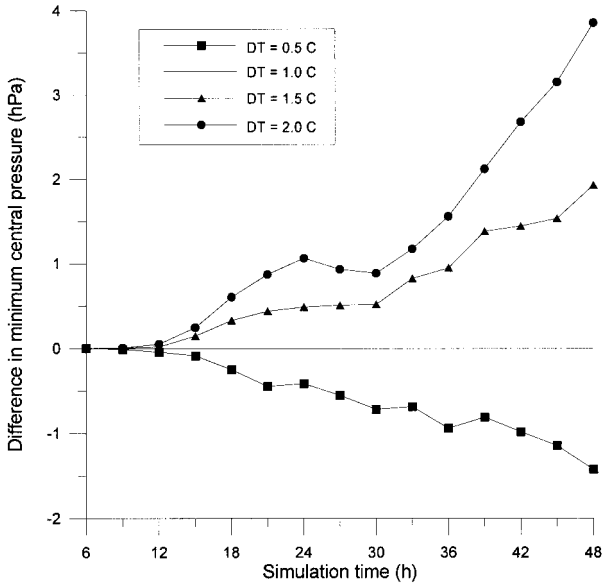

FIG. 11. Time series of the difference in MSLP (hPa) between three experiments [expt. DT1 (DT = 0.5°C), expt. DT2 (DT = 1.5°C), and expt. DT3 (DT = 2.0°C)] and expt. AC (DT = 1.0°C). Value of DT is the temperature difference between the two ocean layers.

1993). Recently, Wu and Wang (1999) have suggested that the movement of a baroclinic vortex in the presence of heating may be related more to potential vorticity advection and heating throughout a deep layer than to the β effect. Since the focus of this paper is on intensity changes rather than track, the physical processes associated with the motion are not investigated further.

The minimum central pressure of the TC decreases rapidly from the beginning to 21 h (Fig. 2). A slight increase in central pressure (of ~6.5 hPa) occurs during the period from 21 to 27 h, which is also found by Hodur (1997). In the next 6 h, the model TC exhibits another rapid deepening phase. The minimum sea level pressure (MSLP) falls from 986 to 927 hPa during the 48-h period.

A marked warm core structure from the surface to the tropopause, with a maximum at $\sigma \approx 0.3$ (about 300 hPa), is also evident (Fig. 3). At each σ level, the temperature deviations are calculated relative to the average temperature of all the grid points along the x direction of the TC center. The general features in Fig. 3 are very similar to those obtained from the multilevel flight observations in Hurricane Inez (1966) (Hawkins and Imbembo 1976) and those simulated by Liu et al. (1997). The maximum deviation in the warm core increases from 8°C at the beginning of the integration (not shown) to over 12°C after 48 h. Notice from Fig. 3 that while the temperature anomalies are largely symmetric at the mid- to low troposphere, obvious asymmetries exist at the upper levels. Such asymmetries may be related to those in the wind fields at these levels (see, e.g., Fig. 5b).

The vertical cross section of the equivalent potential temperature, θ_e, is also similar to that of Liu et al. (1997), despite the relatively coarse resolution of the present model (Fig. 4). The TC intensity, in terms of the MSLP, $P_{\min}$, can be estimated from the maximum θ_e ($\theta_{e\max}$) using the empirical relation of Malkus and Riehl (1960):

$$P_{\min} - P_{\mathrm{E}} = -2.5(\theta_{e\max} - 350),$$

where P_{E} in this study is 1000 hPa. At 48 h, $\theta_{e\max}$ is 378 K at the center. This gives a minimum pressure of 930 hPa, which is close to the simulated 927 hPa in Fig. 2.

The flow at 36 h has strong convergence at $\sigma = 0.99$, the lowest layer of the model (Fig. 5a). Notice that the model produces an asymmetric wind structure. The area of maximum wind speed (>64 m s^{-1}) at this level is ~50 km east-northeast of the TC, while the wind speed is ~6 m s^{-1} at the TC center. The range of 40 m s^{-1} winds is concentrated within a 100-km radius from TC center. These characteristics are similar to the observations of Powell and Houston (1996) and the simulation results of Liu et al. (1997) for Hurricane Andrew (1992).

The vortex exhibits a highly asymmetric flow pattern at the upper levels ($\sigma = 0.08$, about 160 hPa) (Fig. 5b). The flow near the center remains cyclonic but becomes anticyclonic farther out, with the outflow directed toward the southeast. Such an asymmetric structure is common to real TCs (Anthes 1982).

These results demonstrate that the uncoupled version of the model is capable of spinning up an intense hurricane-like vortex when initialized with a relatively weak cyclonic vortex with no background flow and a

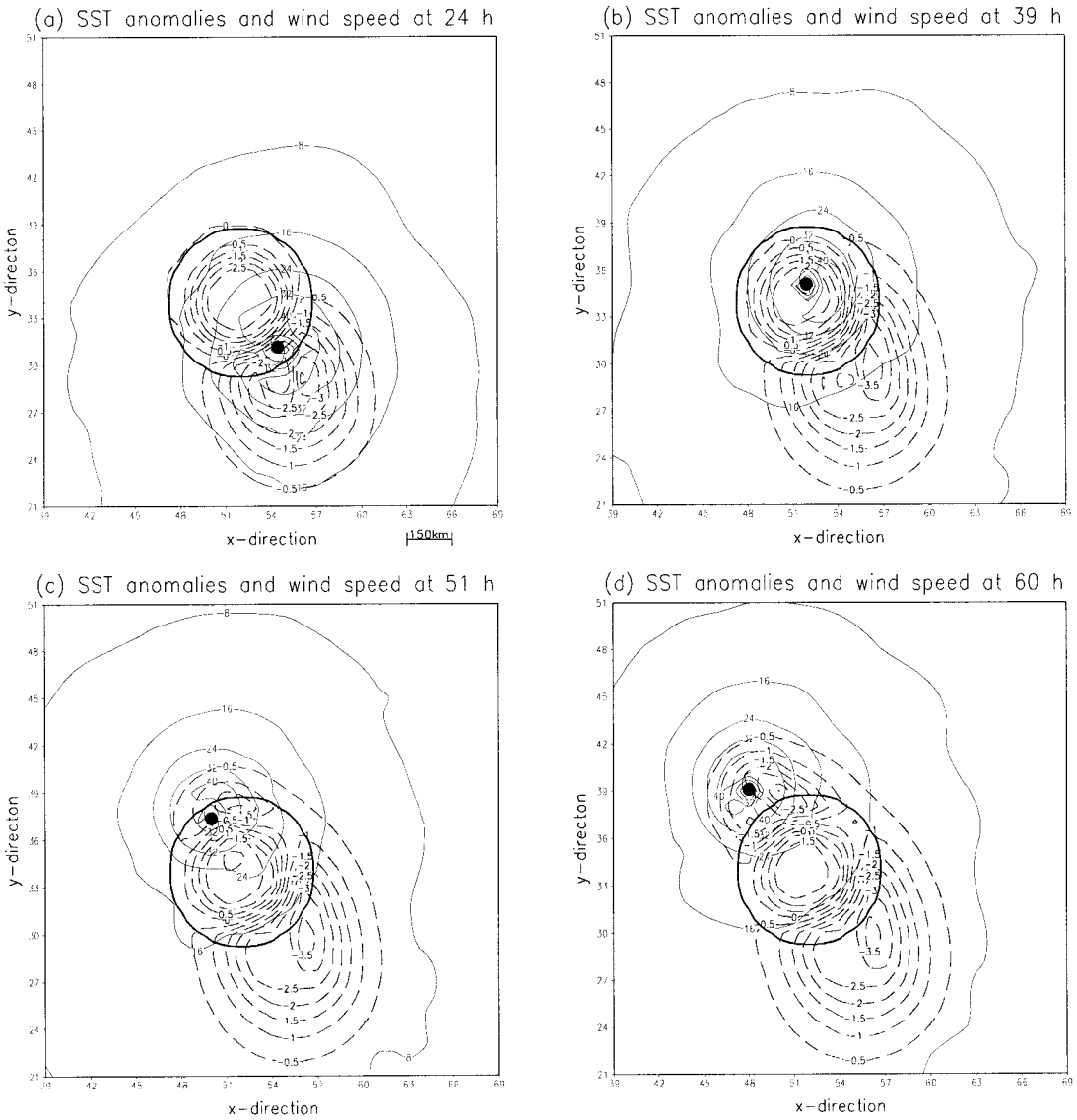

FIG. 12. As in Fig. 7, except for expt. P1 and at (a) 24, (b) 39, (c) 51, and (d) 60 h. The typhoon symbol indicates the center of the TC at the specified time. The thick solid line is the 27.1°C contour corresponding to the boundary of the initial WCE. Contour interval: 8 m s^{-1} (wind), 0.5°C (SST).

fixed SST. The next steps are then to test whether the coupled version can realistically simulate the TC–ocean interaction and how the TC intensity changes in the presence of a mean flow.

b. Coupled run (expt. AC)

The track of the modeled TC in experiment AC is almost identical to that in experiment A0 (see Fig. 1), which suggests that coupling with an initially homogenous ocean does not alter the movement of a TC. As expected, the TC intensity in the coupled model is lower than that in experiment A0 due to the negative feedback from the ocean (Fig. 2). Many previous authors have also discussed such an effect (Ginis and Dikinov 1989; Bender et al. 1993; Hodur 1997). The difference in intensity between the two experiments begins at 6 h, when the coupling is initiated, and increases with time. The effect of coupling becomes obvious after 27 h. By 48 h, the modeled TC in experiment AC is 30 hPa weaker.

The SSTs show a decrease due to the effect of the TC on the ocean, which suggests that the change in SST is significant from 12 to 21 h (Fig. 6). Notice, however, that the SST changes little after 27 h. Compared with the maximum wind speed of the TC, which increases from 6 to 18 h when it reaches 51 m s^{-1}, the SST decrease lags the wind speed increase by more than 6 h. The decrease in maximum wind speed after 21 h is caused by the negative feedback due to upper-ocean cooling. This can also be seen from the MSLP in Fig. 2.

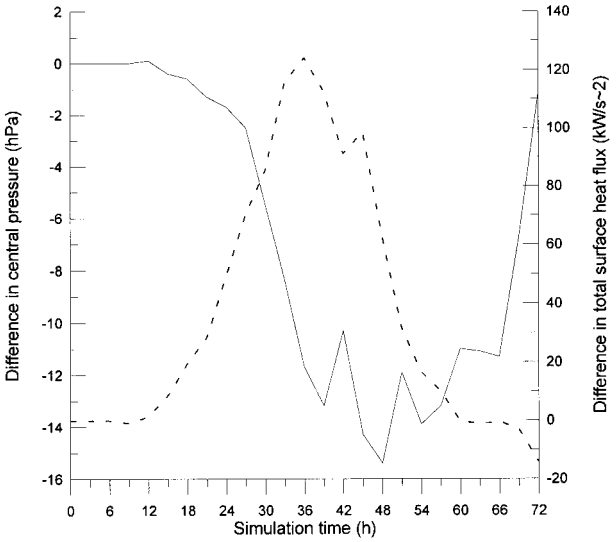

FIG. 13. Time series of differences in central pressure of the TCs between expts. AC and P1 (solid) (negative means pressure is lower in the latter), and deviation of total surface heat flux in the range of 250 km from the TC center between expts. AC and P1 (dashed).

In terms of the horizontal distribution of SST, the area of maximum decrease in SST is in the wake of the TC center (Fig. 7), with a minimum value of 23.4°C after 48 h, which is 3.6°C lower than that of the environment. The distance between the centers of minimum SST and maximum wind increases with time as well. Notice also that the asymmetry in the SST distribution becomes more significant with time. The near collocation of the largest increase in ML depth with the maximum SST decrease (Fig. 8) suggests that the primary physical mechanism is entrainment mixing across the base of the mixed layer (Jacob et al. 2000). A similar asymmetry in the ML depth can also be seen. The asymmetries in the SST and ML probably result from those associated with the TC wind distribution. In fact, the locations of minimum SST and maximum ML largely match that of the maximum wind speed but with a delay in the response time. These results generally agree with those from observational studies (Price 1981; Sanford et al. 1987; Shay et al. 1992) and coupled simulations (e.g., Bender et al. 1993; Hong et al. 2000).

c. *Atmospheric model run with an easterly mean flow (expt. B0)*

Even though the mean flow is purely easterly, the modeled TC has a larger meridional displacement than the case with no mean flow (Fig. 1). Again, the reason for this will not be explored. It suffices to say that this result is consistent with other simulations (e.g., Bender et al. 1993; Peng et al. 1999).

Compared with experiment A0 (no mean flow case), inclusion of a uniform mean flow reduces the TC intensity (Fig. 2). With an easterly mean flow of 5 m s^{-1}, the MSLP only reaches 944 hPa at 48 h (cf. 927 hPa with no basic mean flow). The main difference between the two experiments begins after ~18 h, when the adjustment process is near completion. The reduction in TC intensity under a uniform flow has also been studied in detail by Peng et al. (1999), whose result is consistent with the present one. Other characteristics such as the warm core, vertical distribution of θ_e, and horizontal wind distribution are generally similar to those without a mean flow. These results will therefore not be shown. Thus, it is concluded that the present atmospheric model has the ability of simulating the intensity change in an atmosphere with a mean flow.

In summary, the relatively simple model used in this study appears to be capable of simulating the main characteristics of a TC. In addition, the coupled version of the model correctly simulates the SST decrease induced by the TC, and the minimum central pressure change caused by the negative feedback of the ocean, as well as other features that indicate the interaction between the ocean and the TC. The decrease in TC intensity in the presence of an easterly mean flow is also successfully simulated. These results therefore suggest that the present coupled model can be used to simulate the ocean–TC interaction.

4. Oceanic effects on TC intensity

The experiments in this section are designed to study changes in TC intensity in response to those in SST, ML depth, and vertical ocean temperature structure. A summary of these experiments is listed in Table 2.

a. *Initially uniform oceanic conditions*

1) SST CHANGES

Experiments S1–S6 are designed to study the relationship between TC intensity and SST, which is varied from 25° (S1) to 31°C (S6). The initial SST is 27°C for all the experiments, and the value of the SST is then changed after the atmospheric model has been integrated for 6 h, when the coupled run begins.

The MSLP variations with SST show that the TC responds to an SST change almost instantaneously (Fig. 9). An important result is the nonuniform rate of change in TC intensity per degree change in SST. The change in TC intensity at 48 h is ~−9 hPa $°C^{-1}$ if SST < 27°C (Table 3), but becomes ~16 hPa $°C^{-1}$ when 27°C ≤ SST < 30°C, and then decreases to ~12 hPa $°C^{-1}$ if 30°C ≤ SST ≤ 31°C. Some implications may be drawn from this apparent three-stage change. First, the TC weakens if the SST falls below 27°C, which suggests that the value of 27°C may be considered as a threshold for TC development. While such a result may be fortuitous and may depend on a number of factors in the model formulation, it is nevertheless consistent with the observed requirement that TCs generally do not form

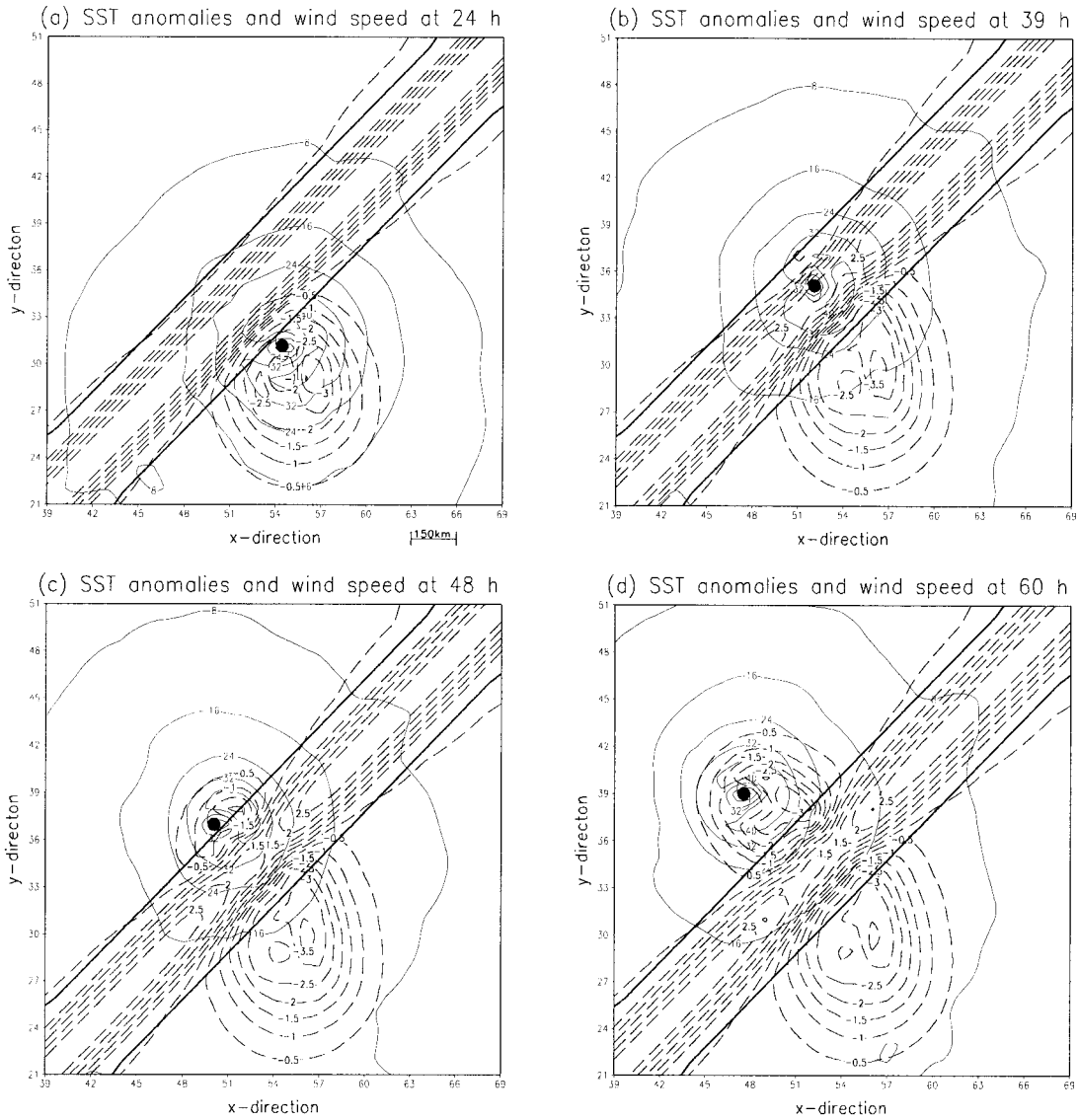

FIG. 14. As in Fig. 7, except for expt. P2 at (a) 24, (b) 39, (c) 48, and (d) 60 h. Typhoon symbol indicates the TC center at the specified time. The thick solid line is the 27.1°C contour corresponding to the boundary of the initial ridge. Contour interval: 8 m s^{-1} (wind), 0.5°C (SST).

over waters with SST $<$ 27°C (Gray 1979). Thus, it might be concluded that an SST in the neighborhood of ~27°C indeed represents a threshold for a TC to develop further. Second, Holland (1997) suggested that, based on the Carnot engine concept of Emanuel (1991), the rate of change of the maximum potential intensity is ~10.5 hPa $°C^{-1}$ between 20° and 31°C (see his Table 2). However, using a thermodynamic approach, he obtained a rate of 33 hPa $°C^{-1}$ when 27°C $\leq$ SST $\leq$ 31°C. The present result is between these two numbers, which appears to be reasonable since the latter approach does not take into consideration dissipation mechanisms, while the former does not include thermodynamic processes within much of the troposphere. Finally, the decrease in the rate of intensification (hPa $°C^{-1}$) when the SST is above 30°C suggests a possible limitation on TC intensification if the forcing is purely thermodynamic and comes only from the lower boundary. More investigation may be necessary in the future to understand this further, but it is beyond the scope of the present study.

2) CHANGES IN ML DEPTH WITH A MEAN BASIC FLOW

It has been shown in section 3c that in a noncoupled model, the presence of an easterly mean flow would reduce the rate of TC intensification. Peng et al. (1999)

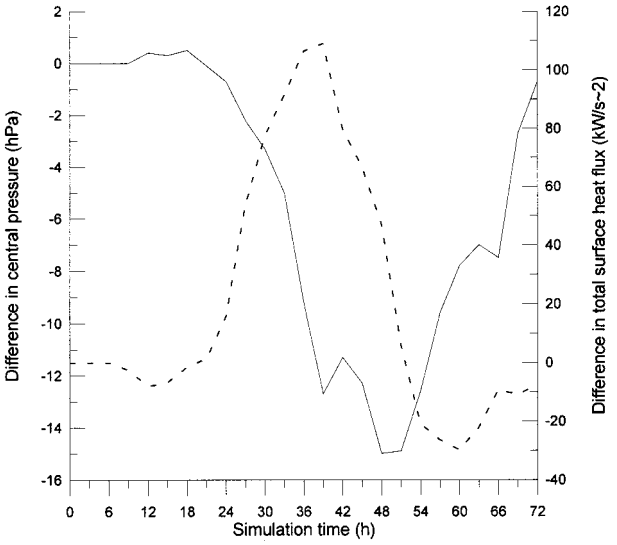

FIG. 15. As in Fig. 13, except for the comparison between expts. P2 and AC.

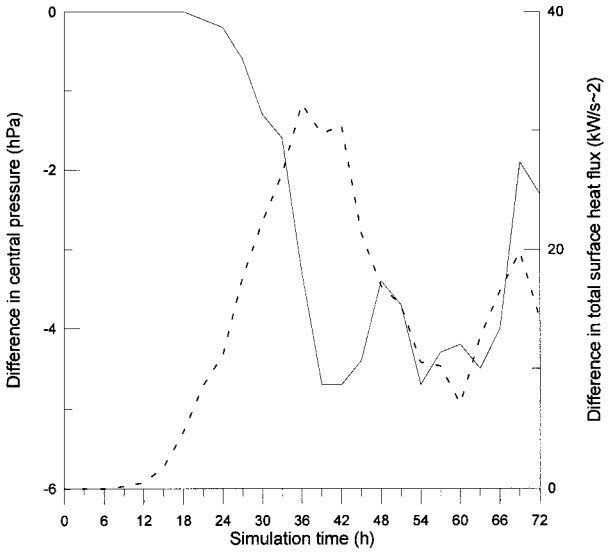

FIG. 16. As in Fig. 13, except for the comparison between expts. P3 and AC.

explained the lesser intensification of the vortex when an easterly flow is present in terms of the enhancement of the ventilation flow from the β effect and the change in surface heat flux distribution. The problem becomes more complicated in a coupled model due to the coupling effect. Nine experiments were designed to study the effect of the ML depth on TC intensity in different easterly flow environments (expts. UM01–UM23; see Table 2).

The effect of ML depth on TC intensity has been shown by previous observational studies (e.g., Jacob 1997; Shay et al. 1998, 2000). The first group of experiments (UM01–UM03) without a mean flow gives a similar result, in that the deeper the ML depth, the more intense the TC becomes (Table 4). For example, an increase of 35 hPa is obtained at 48 h when the ML depth decreases from 100 to 25 m. Note that the change in TC intensity is not linear with the ML depth, and the maximum change occurs when the ML depth changes from 50 to 25 m. This result suggests that changes in TC intensity are more sensitive to change in the ML depth when the latter is <50 m. A similar result is found when an easterly mean flow is present.

The results in Table 4 also suggest that the sensitivity of TC intensity to ML depth depends on the strength of the mean flow. When the ML depth is ≤ 50 m, changes in TC intensity are almost independent of the magnitude of the mean flow. On the other hand, a significant MSLP change ($\sim$6–10 hPa) occurs when the ML depth is ≥ 75 m, and the mean flow changes from 2.5 to 5.0 m s^{-1}.

Similar to the study of Bender et al. (1993), these results can be understood in terms of the sea surface heat flux. The deeper the ML, the more heat is available for the TC to maintain itself or even intensify. Thus, under the same mean flow conditions, the TC intensity increases with ML depth. However, the magnitude of the mean flow has some bearing on the intensity change of the TC. In the presence of a strong advective flow, the TC has less time to be cooled by the ocean, and thus the TC becomes more intense. On the other hand, if the ML is shallow, turbulent mixing events occur over a short period of time, irrespective of the magnitude of the mean flow.

3) CHANGES IN THE VERTICAL STRUCTURE OF THE OCEAN

In the current ocean model, two parameters define the vertical structure of the ocean: the temperature difference between the ML and the stagnant layer below, and the vertical temperature gradient within the latter. In this section, the effects of changes in these two parameters on TC intensity are explored (expts. GM1–GM3 and DT1–DT3; see Table 2).

Physically, the larger the vertical temperature gradient of the stagnant layer, the weaker the TC intensity should be, since more cold water is brought up to the upper mixed layer. Indeed, an increase in such a gradient reduces the rate of intensification (Fig. 10). The response to such a change is almost instantaneous (6 h into model integration, when the coupling begins). Although the TC intensifies by about 5 hPa when the gradient decreases from 0.1° to 0.05°C m^{-1}, it weakens much less when the gradient increases by the same amount. The intensity also changes very little when the gradient varies from 0.2° and 0.15°C m^{-1} (Fig. 10). These results suggest that the effect of the vertical temperature gradient is not linear. The corresponding changes in the SST are also consistent with these intensity changes (not

shown). That is, stronger shear across the base of the mixed layer is required for the layer temperature (density) gradients to lower the Richardson number to below criticality.

For the same reason, an increase in the temperature difference (DT) between the two ocean layers results in a decrease in the MSLP of the TC (Fig. 11). The change in TC intensity with DT is almost linear, with a rate of ~1.5–1.8 hPa for every 0.5°C change in DT.

b. Localized changes in the ocean

In this section, the response of a TC as it encounters a localized region of inhomogeneity in the ocean is examined. Such inhomogeneities include a WCE (expts. P1 and P3) and a sharp gradient of SST (expt. P2).

1) PASSAGE OVER A WCE (EXPT. P1)

Based on the TC track in experiment AC (see Fig. 1), the position (x_0, y_0) at 39 h is chosen as a reference point. For experiment P1, a WCE is set at this location with the SST and the ML depth (H) having the following structure:

$$\mathrm{SST}(r) = \begin{cases} 30 & r \le 100 \text{ km} \\ 30 - 3 \times \left(1 - \dfrac{r - r_0}{100}\right) & \\ & 100 \text{ km} < r \le 200 \text{ km} \\ 27 & r > 200 \text{ km} \end{cases}$$

and

$$H(r) = \begin{cases} 100 & r \le 100 \text{ km} \\ 100 - 50 \times \left(1 - \dfrac{r - r_0}{100}\right) & \\ & 100 \text{ km} < r \le 200 \text{ km} \\ 50 & r > 200 \text{ km}, \end{cases}$$

where r is the distance from one point to the reference point (x_0, y_0).

In experiment P1 (r_0 = 200 km), a change in TC intensity occurs after 12 h (see Fig. 13) because the outer region of the TC has reached the WCE, although the center is still far away (figure not shown). From 12 to 24 h, the TC intensifies slightly as the it moves closer to the WCE (Fig. 12a). From 24 to 39 h, the MSLP decreases by ~11 hPa relative to that in experiment AC (Fig. 13). At this latter time, the TC has moved to the center of the WCE (Fig. 12b). The rate of intensification is ~0.9 hPa h^{-1} during this period. The maximum difference in the MSLP between experiments P1 and AC occurs at 48 h, when it reaches ~15.5 hPa. Although the center of TC has passed the center of WCE by this time, it is still over the WCE, so it continues to intensify. After 48 h, the TC begins to move to the cold water (due to the effect of the TC on the ocean) on the other side of WCE (Fig. 12c). As a result, the TC starts to weaken. The effect of the WCE on the TC remains until 72 h into the integration time, although the TC center has left the WCE at ~54 h. This result underscores the relative importance of the deep and shallow mixed layers in strengthening and weakening of a TC, which tends to be a slow process.

Notice from Fig. 12 that the basic structure of the WCE remains generally unchanged. The maximum SST near the center of the WCE has decreased only by about 1°C. However, two cold water pools have formed around the periphery of the WCE, one along the wake of the TC and the one almost collocated with the region of maximum wind (Fig. 12). Though the background flow was more complicated, and the intensity change obtained here is not as dramatic, to a certain extent this result resembles that of Hurricane Opal when it passed over the Loop Current and warm core ring (Black and Shay 1998; Shay et al. 1998, 2000). Hong et al. (2000) also obtained a similar result from their numerical simulation.

Reasons that the present model TC does not intensify as much as in the case of Opal may include the following. The TC is moving with a speed of 4.5 m s^{-1} from 33 to 42 h, which puts it into the moderate category, according to Black and Shay (1998). Following Greatbatch (1983), the time available for vertical mixing can be expressed as $4R_{\max}/U_h$, where $R_{\max}$ is the radius of the TC, and U_h the propagation speed of the TC. In experiment P1, $R_{\max}$ is ~50 km and U_h is ~4.5 m s^{-1}, so that the time available for vertical mixing is ~12 h, which is much longer than that of Opal (~5 h; Shay et al. 1998, 2000). Such a long mixing time may not be conducive to TC intensification. As a result, the extent of deepening is much less. In addition, although the experiment is designed to have the TC center passing over the center of the WCE, the area of maximum winds is not directly over the area of the highest SST because of the asymmetric structure of TC. Other atmospheric features such as an upper-level trough might also have an appreciable contribution to its intensification (Bosart et al. 1999), which cannot be simulated in the present model.

It should be pointed out that experiment P1 is not designed specifically to simulate the case of Hurricane Opal. The comparison is simply to use the similarity between the simulated results and the observations associated with the intensification of Opal to suggest that the physical processes identified here might also have occurred in the case of Opal.

The total surface (sensible and latent) heat flux in experiment P1 begins to exceed that of experiment AC at 12 h, the time when the TC intensity also increases relative to the latter (Fig. 13). The difference in the heat flux between the two experiments increases as the TC moves toward the center of the WCE, reaching the maximum at 39 h. This is ~9 h prior to the occurrence of

the maximum difference in intensity. Although the difference in total heat flux shown in Fig. 13 is calculated within a radius of 250 km of the TC center, such a time lag is found to be the same for radii between 250 and 500 km (not shown). The profile of the difference in total heat flux is also similar for different radii. More studies of the heat flux will be made in a future paper. Here, it suffices to say that the effect of a WCE is to intensify a TC through the process of enhanced surface heat flux that begins to occur *prior to* the arrival of the TC center at the WCE. Such a result will have implications on the operational forecasting of intensity change.

2) PASSAGE OVER A SHARP GRADIENT OF SST (EXPT. P2)

The sharp gradient of SST in experiment P2 is defined as a narrow strip of warm water with the following structure:

$$\mathrm{SST}(r) = \begin{cases} 30 & r \le 50 \text{ km} \\ 30 - 3 \times \left(1 - \dfrac{r - r_0}{50}\right) & \\ & 50 \text{ km} < r \le 100 \text{ km} \\ 27 & r > 100 \text{ km} \end{cases}$$

and

$$H(r) = \begin{cases} 100 & r \le 50 \text{ km} \\ 100 - 50 \times \left(1 - \dfrac{r - r_0}{50}\right) & \\ & 50 \text{ km} < r \le 100 \text{ km} \\ 50 & r > 100 \text{ km}, \end{cases}$$

where r is the distance from one point to the line $y - y_0 = k(x - x_0)$, and k is the slope of the warm ridge. The value of r_0 is set at 100 km.

Although the change in TC intensity is this case appears to be roughly the same as that of passage over a WCE (cf. Figs. 13 and 15), some important differences exist. When the TC first starts to move over the sharp gradient from the 9 to 21 h, the TC actually weakens slightly (see Fig. 15) because the cool water induced by the TC piles up to the southeast of the warm ridge (Fig. 14a). As a result, the difference in total surface heat flux between this case and experiment AC is negative (Fig. 15). The TC then begins to intensify (at around 21 h) as it moves closer to the warm ridge, which results in a positive upward heat flux. The evolution of the vortex subsequently becomes similar to the case of experiment P1, until around 51 h, when the heat flux again becomes negative relative to experiment AC (Fig. 15). The TC weakens dramatically when it is located over the cool water on the other side of the warm ridge that is induced by the TC circulation (Fig. 14d).

These two experiments suggest that the ocean surface and subsurface structure can play a significant role in modifying the intensity of a TC. Further, the changes in TC intensity occur before the TC center reaches the boundary of the inhomogeneity and can continue after it leaves the anomalous temperature and current structure of the ocean.

3) PASSAGE OVER A WCE WITH A HOMOGENOUS SST (EXPT. P3)

A warm core eddy in the ocean may have both an above-normal SST as well as a deep ML. Therefore, another experiment (expt. P3; $r_0 = 200$ km) is designed to investigate the effect of the ML depth on TC intensity in such a case. To isolate this effect, the initial SST is defined to be homogenous (with a value of 27°C), while the ML depth has the same structure as that in experiment P1. The difference in intensity between experiments P3 and AC occurs after 18 h, when the TC center first reaches the deep ML regime (Fig. 16). This also corresponds to the time when the difference of total surface heat flux between the two experiments is positive. The maximum difference in MSLP is ~5 hPa, which is much less than that in experiment P1 (see Fig. 13). This numerical result therefore suggests that a locally deep ML can only produce a slight intensification.

5. Summary and discussion

a. Summary

In this study, the problem of tropical cyclone–ocean interaction is investigated using an atmosphere–ocean coupled model. The coupled model is developed from the Penn State/NCAR mesoscale model version 4 (MM4) and an oceanic mixed layer model. Coupling between the atmosphere and the ocean is achieved through the wind stress. The subsequent SST calculated from the ocean model is then fed back into the atmosphere. The control experiment demonstrates that the coupled model has the ability to simulate the interaction between a TC and its underlying ocean.

The response of a TC to changes in SST is found to be almost instantaneous. A critical SST of around 27°C is apparently necessary for a TC to intensify, which agrees well with previous observational results. Intensification proceeds most rapidly when the SST is between 27° and 30°C but slows down as the SST increases above 30°C.

A change in initial ML depth also has a significant effect on TC intensity. Generally speaking, the deeper the ML, the more intense the TC may become given its translation speed. In addition, changes in TC intensity are more sensitive to the ML depth when the latter is <50 m, irrespective of whether an easterly flow is present. However, a strong easterly flow will tend to reduce the rate of intensification, especially when the ML is deep.

In addition to the ML depth, changes in the other parameters related to the vertical structure of the ocean can also modify the rate of intensification. An increase in the vertical temperature gradient in the stagnant layer is not conducive to TC intensification, although the relationship between the two processes is not linear. A larger differential in temperatures between the upper and lower layers also results in a lesser intensification.

When a TC passes over a warm core eddy, the TC intensifies prior to reaching the center of the WCE. Further, as the TC exits the WCE regime, the weakening process does not occur immediately. Although the SST near the center of the WCE changes only slightly, and the WCE generally maintains its original characteristics, two cold pools form around the periphery of the WCE, one to the wake of the TC and the other located underneath the area of maximum winds of the TC. A similar intensification process occurs when a TC moves over a localized area of deep ocean mixed layer, though to a lesser extent. When a TC passes over a sharp SST gradient, changes in TC intensity resemble those in the case of the passage over a WCE, although some differences exist in terms of the total surface heat flux changes.

b. Discussion

Comparing the results obtained by different ocean–atmosphere coupled models is difficult because the physical processes and parameterizations in each model can be vastly different. For example, Bender et al. (1993) ran a coupled model without an initial basic flow and obtained a maximum SST anomaly of about −5.6°C, the corresponding increase in MSLP being 16.4 hPa. On the other hand, Hodur (1997) reported an 8°C decrease in SST and a 55-hPa increase in MSLP from his coupled model run for a stationary vortex. The present study indicates an MSLP increase of 30 hPa and an SST decrease of 3.6°C. Nevertheless, the qualitative conclusion that the oceanic thermodynamic properties have a significant effect on TC intensity is consistent with observational and numerical studies (Shay et al. 2000; Hong et al. 2000).

The contribution from this study is that localized variations of ocean conditions can lead to changes in TC intensity. The experimental results reveal that the effect of the ocean occurs a long time before the TC reaches such a localized anomaly. The total (latent and sensible) heat flux decrease appears to be the most likely mechanism, which has been identified by Bender et al. (1993) as the major physical process when a TC is coupled with the ocean. They also found that the sensible heat transport is from the atmosphere to the ocean, which means that the latter is actually cooler. Combined observational and numerical studies of this mechanism are necessary to verify these results.

Other than the direct effects of the ocean, other processes, such as wind–wave interaction and cooling due to evaporation of sea spray, may also contribute to changes in TC intensity. However, these are probably second-order effects at most. While their contributions may modify the absolute rates of intensity change, the conclusions based on the results of this study will still be valid.

In addition to ocean conditions, the atmosphere can also induce changes in TC intensity (see, e.g., Holland 1987) or at least provide favorable conditions for rapid intensification to occur (Bosart et al. 1999). Shay et al. (2000) argues that upper-ocean effects and atmospheric processes may have a phase lock when these rapid intensifiers occur. That is, the oceanographic and atmospheric factors may not be independent of one another, and one has to be careful about the extent of positive versus negative feedback between the ocean and atmosphere. Therefore, it is important to study TC intensity changes in a coupled model to understand the effects between the atmosphere and the ocean. This study demonstrates that a simple model with even a relatively coarse resolution can simulate the major features of the TC–ocean interaction, so that such a model can be utilized for future studies of TC–ocean interaction.

Acknowledgments. The authors would like to thank the Shanghai Typhoon Institute, China, for providing the code for the coupled model. The first author was a Croucher Foundation Senior Research Fellow and was on sabbatical leave at the Naval Postgraduate School and the University of Hawaii during part of this study. Comments from Prof. R. L. Elsberry on an earlier version of the manuscript are greatly appreciated. This research was sponsored by the Strategic Research Grant 7000836 of the City University of Hong Kong and partly by the Office of Naval Research Grant N00014-94-1-0824. Lynn K. Shay was supported by the National Science Foundation (ATM-97-14885) and the U.S. Naval Research Laboratory (N00014-96-G904) in the preparation of this manuscript.

APPENDIX

Comparison of the Rates of Intensification between Two Cumulus Parameterization Schemes

Version 5 of the Penn State/NCAR mesoscale model (MM5) is coupled with the same ocean model described in the main text in this comparison. The initial vortex is the same as that described in section 2a. Three sets of experiments have been carried out using SST values of 28°, 29°, and 30°C. In each set, two experiments are performed, one using the Kuo scheme and the other using the Betts–Miller scheme. It can be seen in Fig. A1 that for the same increase in SST, the decrease in central pressure is very similar between the two schemes. In other words, the effect of the SST on the relative rates of intensification is largely independent of the cumulus parameterization schemes.

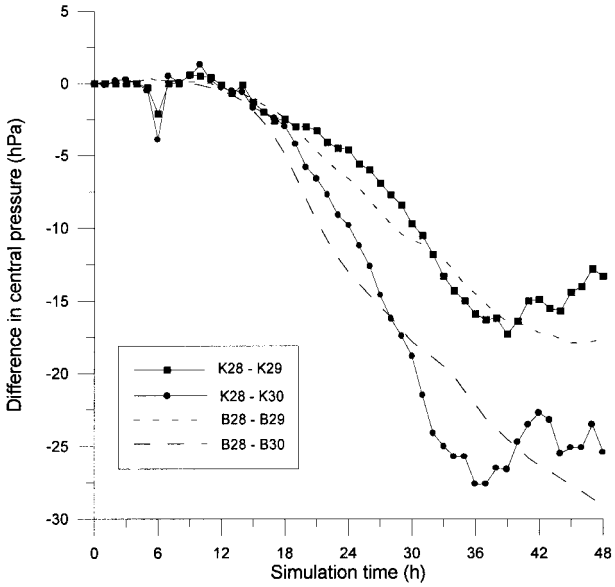

FIG. A1. Time series of the difference in minimum surface pressure at the TC center between various experiments. K28–K29 (K28–K30) indicates the difference in experiments with SSTs equal to 28° and 29° (28°C and 30°C) using the Kuo parameterization scheme. Experiments using the Betts–Miller scheme are indicated with B.

REFERENCES

Anthes, R. A., 1977: A cumulus parameterization scheme utilizing a one-dimensional cloud model. *Mon. Wea. Rev.*, **105,** 270–286.

——, 1982: *Tropical Cyclones: Their Evolution, Structure and Effects, Meteor. Monogr.*, No. 41, Amer. Meteor. Soc., 208 pp.

——, E.-Y. Hise, and Y.-H. Kuo, 1987: Description of the Penn State/NCAR mesoscale model version 4 (MM4). NCAR Tech. Note NCAR/TN-282, 66 pp. [Available from Dr. J. C.-L. Chan, Dept. of Physics and Materials Science, City University of Hong Kong, 83 Tat Chee Ave., Kowloon, Hongkong, China.]

Bender, M. A., I. Ginis, and Y. Kurihara, 1993: Numerical simulation of tropical cyclone-ocean interaction with a high-resolution coupled model. *J. Geophys. Res.*, **98,** 23 245–23 263.

Black, P. G., and L. K. Shay, 1998: Observations of the tropical cyclone intensity change due to air–sea interaction processes. Preprints, *Symp. on Tropical Cyclone Intensity Change*, Phoenix, AZ, Amer. Meteor. Soc., 161–168.

Bosart, L. F., W. E. Bracken, J. Molinari, C. S. Velden, and P. G. Black, 1999: Environmental influences on the rapid intensification of Hurricane Opal (1995) over the Gulf of Mexico. Preprints, *23d Conf. on Hurricanes and Tropical Meteorology*, Dallas, TX, Amer. Meteor. Soc., 983–984.

Brown, J., and K. Campana, 1978: An economical time-differencing system for numerical weather prediction. *Mon. Wea. Rev.*, **106,** 1125–1136.

Chan, J. C.-L., and R. T. Williams, 1987: Analytical and numerical studies of the beta-effect in tropical cyclone motion. Part I: Zero mean flow. *J. Atmos. Sci.*, **44,** 1257–1265.

Chang, S. W., and R. A. Anthes, 1978: Numerical simulation of ocean's nonlinear, baroclinic response to translating hurricanes. *J. Phys. Oceanogr.*, **8,** 468–480.

Deardorff, J. W., 1972: Parameterization of the planetary boundary layer for use in general circulation models. *Mon. Wea. Rev.*, **100,** 93–106.

DeMaria, M., and J. D. Pickle, 1988: A simplified system of equations for the simulation of tropical cyclones. *J. Atmos. Sci.*, **45,** 1542–1554.

Elsberry, R. L., T. Fraim, and R. Trapnell, 1976: A mixed layer model of the ocean thermal response to hurricanes. *J. Geophys. Res.*, **81,** 1153–1162.

Emanuel, K. A., 1988: The maximum intensity of hurricanes. *J. Atmos. Sci.*, **45,** 1143–1155.

——, 1991: The theory of hurricanes. *Annu. Rev. Fluid Mech.*, **23,** 179–196.

Fujita, T., 1952: Pressure distribution in typhoons. *Geophys. Mag.*, **23,** 437–452.

Ginis, I., and Kh. Zh. Dikinov, 1989: Modeling of the Typhoon Virginia (1978) forcing on the ocean. *Sov. Meteor. Hydrol. Engl. Transl.*, **7,** 53–60.

——, ——, and A. P. Khain, 1989: A three-dimensional model of the atmosphere and the ocean in the zone of a typhoon. *Dokl. Akad. Nauk. USSR*, **307,** 333–337.

Gray, W. M., 1979: Hurricanes: Their formation, structure, and likely role in the tropical circulation. *Meteorology over the Tropical Oceans*, D. B. Shaw, Ed., Royal Meteorological Society, 155–199.

Greatbatch, R. J., 1983: On the response of the ocean to a moving storm: The nonlinear dynamics. *J. Phys. Oceanogr.*, **13,** 357–367.

Hawkins, H. F., and S. M. Imbembo, 1976: The structure of a small, intense hurricane—Inez 1966. *Mon. Wea. Rev.*, **104,** 418–442.

Heming, J. T., J. C. L. Chan, and A. M. Radford, 1995: A new scheme for the initialisation of tropical cyclones in the U.K. Meteorological Office Global Model. *Meteor. Appl.*, **2,** 171–184.

Hodur, R., 1997: The Naval Research Laboratory's Coupled Ocean/Atmosphere Mesoscale Prediction System (COAMPS). *Mon. Wea. Rev.*, **125,** 1414–1430.

Holland, G. J., 1987: Mature structure and structure change. *A Global View of Tropical Cyclones*, R. L. Elsberry, Ed., University of Chicago Press, 13–52.

——, 1997: The maximum potential intensity of tropical cyclones. *J. Atmos. Sci.*, **54,** 2519–2541.

——, and R. T. Merrill, 1984: On the dynamics of tropical cyclone structure changes. *Quart. J. Roy. Meteor. Soc.*, **110,** 725–745.

Hong, X., S. W. Chang, S. Raman, L. K. Shay, and R. Hodur, 2000: The interaction between Hurricane Opal (1995) and a warm core ring in the Gulf of Mexico. *Mon. Wea. Rev.*, **128,** 1347–1365.

Jacob, S. D., 1997: Effects of oceanic mesoscale variability on SST response: Implication for intensity change. Preprints, *22d Conf. on Hurricanes and Tropical Meteorology*, Fort Collins, CO, Amer. Meteor. Soc., 435–436.

——, L. K. Shay, A. J. Mariano, and P. G. Black, 2000: The 3D oceanic mixed layer response to Hurricane Gilbert. *J. Phys. Oceanogr.*, **30,** 1407–1429.

Kato, H., and O. M. Phillips, 1969: On the penetration of a turbulent layer into stratified fluid. *J. Fluid Mech.*, **37,** 634–655.

Khain, A. P., 1988: Three-dimensional numerical model of a tropical cyclone including β-drift. *Atmos. Ocean Phys.*, **24,** 359–366.

Kuo, H.-L., 1974: Further studies of the parameterization of the influence of cumulus convection on large-scale flow. *J. Atmos. Sci.*, **31,** 1232–1240.

Kurihara, Y., M. A. Bender, and R. J. Ross, 1993: An initial scheme of hurricane model by vortex specification. *Mon. Wea. Rev.*, **121,** 2030–2045.

Liu, K.-S., and J. C.-L. Chan, 1999: Size of tropical cyclone as inferred from ERS-1 and ERS-2 data. *Mon. Wea. Rev.*, **127,** 2992–3001.

Liu, Y., D. Zhang, and M. K. Yau, 1997: A multiscale numerical study of Hurricane Andrew (1992). Part I: Explicit simulation and verification. *Mon. Wea. Rev.*, **125,** 3073–3093.

Malkus, J. S., and H. Riehl, 1960: On the dynamics and energy transformations in steady-state hurricanes. *Tellus*, **12,** 1–20.

Molinari, J., and D. Vollaro, 1990: External influences on hurricane intensity. Part II: Vertical structure and response of the hurricane vortex. *J. Atmos. Sci.*, **47,** 1902–1918.

Peng, M. S., B.-F. Jeng, and R. T. Williams, 1999: A numerical study on tropical cyclone intensification. Part I: Beta effect and mean-flow effect. *J. Atmos. Sci.*, **56,** 1404–1423.

Powell, M. D., and S. H. Houston, 1996: Hurricane Andrew's landfall in Florida. Part II: Surface wind field and potential real-time application. *Wea. Forecasting,* **11,** 329–349.

Price, J. F., 1981: Upper ocean response to a hurricane. *J. Phys. Oceanogr.,* **11,** 153–175.

Qin, Z.-H., and J.-R. Zhu, 1995: Numerical study on nonlinear interaction between tropical cyclone and sea. *Acta Meteor. Sin.,* **9,** 13–25.

Raymond, D., and K. Emanuel, 1993: The Kuo cumulus parameterization. *The Representation of Cumulus Convection in Numerical Models, Meteor. Monogr.,* No. 46, Amer. Meteor. Soc., 145–147.

Ross, R. J., and Y. Kurihara, 1995: A numerical study on influences of Hurricane Gloria (1985) on the environment. *Mon. Wea. Rev.,* **123,** 332–346.

Sanford, T. B., P. G. Black, J. R. Haustein, J. W. Feeney, G. Z. Forristall, and J. F. Price, 1987: Ocean response to a hurricane. Part I: Observations. *J. Phys. Oceanogr.,* **17,** 2065–2083.

Shay, L. K., P. G. Black, A. J. Mariano, J. D. Hawkins, and R. L. Elsberry, 1992: Upper ocean response to Hurricane Gilbert. *J. Geophys. Res.,* **97,** 20 227–20 248.

——, G. J. Goni, F. D. Marks, J. J. Cione, and P. G. Black, 1998: Role of warm ocean features on intensity change: Hurricane Opal. Preprints, *Symp. on Tropical Cyclone Intensity Change,* Phoenix, AZ, Amer. Meteor. Soc., 131–138.

——, G. J. Goni, and P. G. Black, 2000: Role of a warm ocean feature on Hurricane Opal. *Mon. Wea. Rev.,* **128,** 1366–1383.

Sutyrin, G. G., and A. P. Khain, 1979: Interaction of ocean and the atmosphere in the area of moving tropical cyclone. *Dokl. Akad. Nauk. USSR,* **249,** 467–470.

Wang, W., and N. Seaman, 1997: A comparison study of convective parameterization schemes in a mesoscale model. *Mon. Wea. Rev.,* **125,** 252–278.

Willoughby, H. E., and P. G. Black, 1996: Hurricane Andrew in Florida: Dynamics of a disaster. *Bull. Amer. Meteor. Soc.,* **77,** 543–549.

Wu, L., and B. Wang, 1999: Numerical study of tropical cyclone propagation in the presence of diabatic heating. Preprints, *23d Conf. on Hurricanes and Tropical Meteorology,* Dallas, TX, Amer. Meteor. Soc., 91–94.

Zhu, J., 1994: The interaction study between ocean and tropical cyclone (in Chinese). Ph.D. dissertation, Ocean University of Qingdao, 201 pp. [Available from Dr. J. C. L. Chan, Department of Physics and Materials Science, City University of Hong Kong, 83 Tat Chee Ave., Kowloon, Hong Kong, China.]